Mechanisms underlying ferromagnetism across the metal-insulator transition in $La_{1-x}Ca_xMnO_3$

Wanjun Jiang,* X. Z. Zhou, and Gwyn Williams
Department of Physics and Astronomy, University of Manitoba, Winnipeg, Manitoba, Canada R3T 2N2

R. Privezentsev and Y. Mukovskii
State Technological University "Moscow Steel and Alloys Institute" (MISIS), Moscow 119049, Russia
(Received 16 January 2009; revised manuscript received 29 April 2009; published 26 June 2009)

Detailed measurements of the magnetic and transport properties of the two $La_{1-x}Ca_xMnO_3$ ($x=0.18$, $x=0.20$) single crystals straddling the compositional metal-insulator transition boundary ($0.18 \leq x_c \leq 0.22$) are summarized. The analysis of magnetization/susceptibility data reveals the occurrence of a second-order/continuous ferromagnetic-paramagnetic phase transition described not only by nearest-neighbor three-dimensional Heisenberg-model exponents ($\gamma=1.387$, $\beta=0.365$, $\delta=4.783$) but also with comparable values of the critical temperatures and amplitudes in both the insulating and the metallic samples. The implications of these results in terms of the universality class, the percolation thresholds, and the relative magnitudes of the super-exchange and double-exchange interactions underlying ferromagnetism across this compositionally modulated metal-insulator boundary in this system are discussed.

DOI: 10.1103/PhysRevB.79.214433 PACS number(s): 75.40.Cx, 75.47.Gk, 75.47.Lx

I. INTRODUCTION

The presence of metal-insulator (M-I) transitions in magnetic materials, particularly in colossal magnetoresistive (CMR) manganese perovskite manganites,[1–5] have been the focus of intensive study. The general formula for the latter is usually given as $A_{1-x}B_xMnO_3$, x being the doping level, A =rare earth, viz., La, Pr, etc., while B=a divalent alkaline-earth ion, typically Ca or Sr. Historically, the explanation of CMR in manganites was based on the concept of spin-dependent double exchange (DE) (Ref. 6) in which a ferromagnetic (FM) interaction between the localized t_{2g} spins resulted from the hopping of itinerant e_g spins between adjacent Mn atoms subject to strong intrasite Hund's rule coupling. A specific prediction of the conventional DE picture was that the onset of metallicity reflected the establishment of an infinite (percolating) pathway of DE metallic bonds with these same bonds establishing an infinite FM "backbone," so that the emergence of metallicity and ferromagnetism were coincident. Current studies are at variance with such a prediction; in $La_{1-x}Ca_xMnO_3$, for example,[7–9] for doping levels $0.18 \leq x_c \leq 0.22$ (i.e., carrier concentration $n=1-x$), a FM ground state persists but is accompanied alternatively by conducting ($x \sim 0.22$) or insulating ($x \sim 0.18$) characteristics. Recent experiments indicate that the emergence of an insulating, as opposed to a metallic, ground state reflects local structural changes [which control carrier (e_g) (de)localization[10]]. This situation can be characterized quantitatively by the absence/presence of the so-called Jahn-Teller (JT) long bond accompanied by an orbitally ordered (OO) (insulator) to orbitally disordered (OO*) (metal) transition.[10] The origin of ferromagnetism in this composition range thus remains elusive, if not controversial. While quantitative correlations between JT distortions and both the transport and magnetic responses across this compositional phase boundary have been established experimentally,[11] differences in spin excitation processes, viz., the appearance of spin diffusive modes in metallic samples but their absence in the insulating regime, indicate that the associated magnetism *might* be different.[8] Theoretically, the emergence of a FM insulating phase is not a universal model prediction.[12]

The present study attempts to address the failure of the DE model in its prediction for the coincident emergence of ferromagnetism and metallicity in the $La_{1-x}Ca_xMnO_3$ system via measurements of the critical exponents, temperatures, and amplitudes across the compositionally controlled M-I boundary.

II. EXPERIMENTAL DETAILS

Data on two $La_{1-x}Ca_xMnO_3$ single crystals with $x=0.18$ and 0.20, grown using the floating zone technique,[13] are summarized below. Their high structural/magnetic quality is confirmed by a mosaicity typically less than 1° and low coercive fields (at 10 K, $H_C=35$ Oe for $x=0.18$ while $H_C=8$ Oe at $x=0.20$). Measurements of the ac susceptibility, $\chi(H,T)$, (at 1 kHz with an ac driving field of 0.1 Oe rms) and magnetization, $M(H,T)$, were carried out in a Quantum Design Physical Property Measurement System (PPMS) model 6000 susceptometer/magnetometer, with all fields applied along the largest sample dimension to minimize demagnetization effects. Magnetoresistivities, $\rho(H,T)$, were acquired with a Model 7000 ac transport controller using a four-probe technique with an excitation current 10 μA at 499 Hz.

III. RESULTS AND DISCUSSION

Figure 1(a) ($x=0.18$) and Fig. 1(b) ($x=0.20$) reproduce magnetic isotherms at selected temperatures. The insets display the corresponding zero-field ac susceptibilities, $\chi(0,T)$, measured (in 1 K steps) on warming [no hysteresis was detected between cooling and warming through the transition region; the structural phase transition near $T_B \approx 50$ K for $0.125 \leq x \leq 0.20$ (Ref. 8) not being a focus of the present study]. The Hopkinson/principal maxima[14] evident in these insets yield an estimate for the demagnetization factors (N_D), and the inflection points yield a preliminary determination of

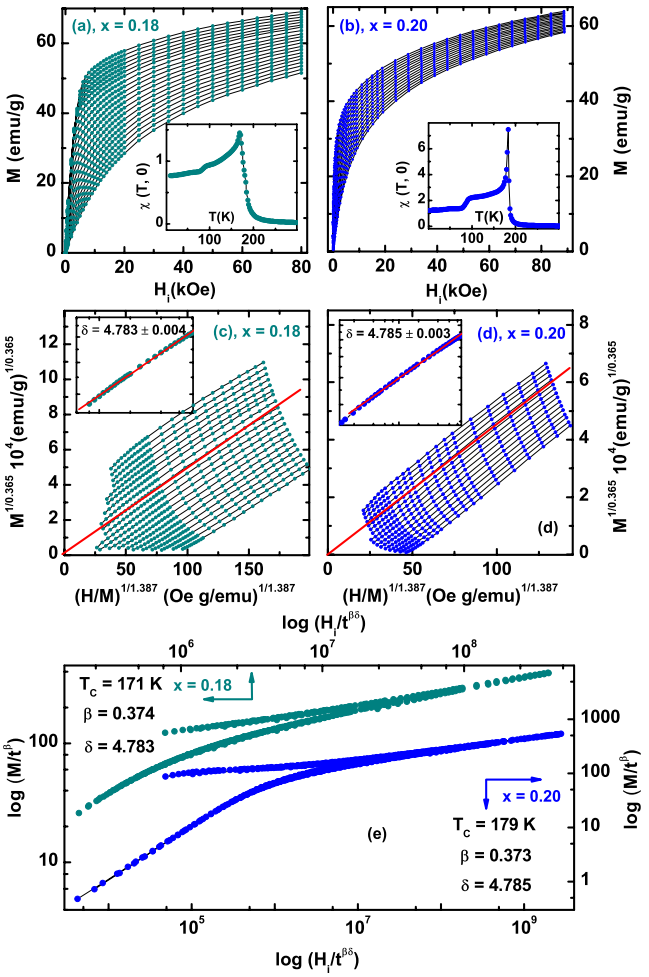

FIG. 1. (Color online) Main body of (a) and (b) is a series of selected magnetic isotherms: (a) $x=0.18$, collected in increasing field from 150 (top) to 190 K (bottom) in 2 K steps; (b) $x=0.20$, collected from 175 (top) to 195 K (bottom) in 1 K steps. The insets in (a) and (b) are the zero-field ac susceptibility $\chi(0,T)$. (c) and (d) reproduce the data in (a) and (b) in the form $(H_i/M)^{1/1.387}$ versus $M^{1/0.365}$. The linear fits to the isotherm passing through the origin yield T_C. The insets are plots of $\log[M(H_i,T=T_C)]$ vs $\log(H_i)$, yielding δ using data in the range of $2<H_i<80$ kOe. (e) Scaling plot of $\log(M/t^{\beta})$ vs $\log(H_i/t^{\beta\delta})$, using the exponents and T_C values deduced above. The upper branch corresponds to data below T_C and the lower branch to data above T_C.

$T_C \approx 171$ K for $x=0.18$ and $T_C \approx 179$ K for $x=0.20$. Magnetization isotherms in the vicinity of these transition temperatures display no S-shaped features characteristic of a metamagnetic/discontinuous transition,[15–17] the continuous nature of the transitions being confirmed by the positive slope of the corresponding Arrott plots.[15] These magnetization (M) data are reproduced in the form $(H_i/M)^{1/1.387}$ vs $M^{1/0.365}$ (here the internal field $H_i=H_a-N_DM$, H_a being the applied field) suggested by a modified Arrott-Noakes equation of state[16] in Fig. 1(c) ($x=0.18$) and Fig. 1(d) ($x=0.20$). The resulting parallel lines confirm the applicability of isotropic near-neighbor three-dimensional (3D) Heisenberg-model exponents [$\gamma=1.387$, $\beta=0.365$, and $\delta=4.783$ (Ref. 18)], and yield values of $T_C \approx 171 \pm 1$ K ($x=0.18$) and $T_C \approx 179 \pm 1$ K ($x=0.20$) from the critical isotherms. Along the latter, standard scaling theory predicts[14–16] $M(H_i,T=T_C)=D_0H_i^{1/\delta}$, where D_0 is a critical amplitude that measures the number of spins involved in the ordering process.[19] This power-law prediction is verified by the double-logarithmic plots inserted in these figures that, further, yield $\delta=4.783\pm0.004$, $D_0=5.4\pm0.1$ emu/g Oe ($x=0.18$) and $\delta=4.785\pm0.003$, $D_0=5.2\pm0.1$ emu/g Oe ($x=0.20$). These δ estimates are not only in close agreement with 3D Heisenberg-model predictions but they also confirm—albeit indirectly—the absence of Griffiths phase-type (GP-type) features (Ref. 20). Separate tests of the power-law predictions for the inverse initial susceptibility $1/\chi_i(T>T_C)=(\partial H/\partial M)_{H=0}=\chi_0|t|^{\gamma}$ and the spontaneous magnetization $M_S(H=0,T<T_C)=M_S(0)|t|^{\beta}$ (where $|t|=|T/T_C-1|$) yield critical amplitudes $\chi_0=(8.9\pm0.5)\times10^3$ g Oe/emu, $M_S(0)=124\pm4$ emu/g ($x=0.18$) and $\chi_0=(1.11\pm0.06)\times10^4$ g Oe/emu, $M_S(0)=132\pm3$ emu/g ($x=0.20$). These power-law plots are not reproduced here, although a final assessment of scaling behavior, viz., $M(H_i,t)=|t|^{\beta}F_{\pm}[H_i/(|t|^{\beta\delta})]$, where $F_{\pm}(x)$ is the (unknown) scaling function above (+)/below(−) T_C,[14,17,20,21] is carried out in Fig. 1(e) using the listed exponent values. The good data collapse evident in this figure confirms the applicability of 3D Heisenberg exponents to both metallic and insulating single crystals. Estimates of the low-temperature spontaneous magnetization, M_S, can be obtained from the intercepts of plots similar to those shown in Figs. 1(c) and 1(d). These enable values for the acoustic spin-wave stiffness, D, to be found using the well-established Bloch $T^{3/2}$ law:[22] fits to the latter indicate $D\sim65$ meV Å^2 in both samples, consistent with the previous results on Ca-doped samples showing no evidence of GP-type features.[4,8,20] Estimates of the saturation and spontaneous magnetizations, M_{sat} and M_S, respectively, at 2 K have been used to verify the nominal composition of these samples by comparing the latter with the theoretically predicted spin-only moment of $(4-x)$ μ_B/Mn. Such estimates yield

$$M_{sat}(T=2\ \text{K}) \approx M_S(T=2\ \text{K}) = 94.8 \pm 0.3\ \text{emu/g} = 3.63 \pm 0.03\ \mu_B/\text{Mn}$$

for $x=0.18$ and

$$M_{sat}(T=2\ \text{K}) \approx M_S(T=2\ \text{K}) = 95.5 \pm 0.4\ \text{emu/g} = 3.60 \pm 0.02\ \mu_B/\text{Mn}$$

for $x=0.20$. Both estimates imply that here the e_g electrons are fully spin polarized with no significant spin canting.[8,23]

ac susceptibility data are in complete agreement with the above conclusions. Figure 2(a) ($x=0.18$) and Fig. 2(b) ($x=0.20$) show that in static-biasing fields, H_a, a series of critical susceptibility maxima emerge. The temperature (T_m) of these peaks increases while the amplitude $[\chi(H_a,T_m)]$ decreases as H_a is increased. The insets of these figures show the inverse zero-field ac susceptibilities $[1/\chi(0,T)]$, in which the lack of a characteristic downturn just above T_C provides convincing evidence regarding the absence of GP-type features[20] in these samples. The evolution of the critical maxima mentioned above with field and temperature, in

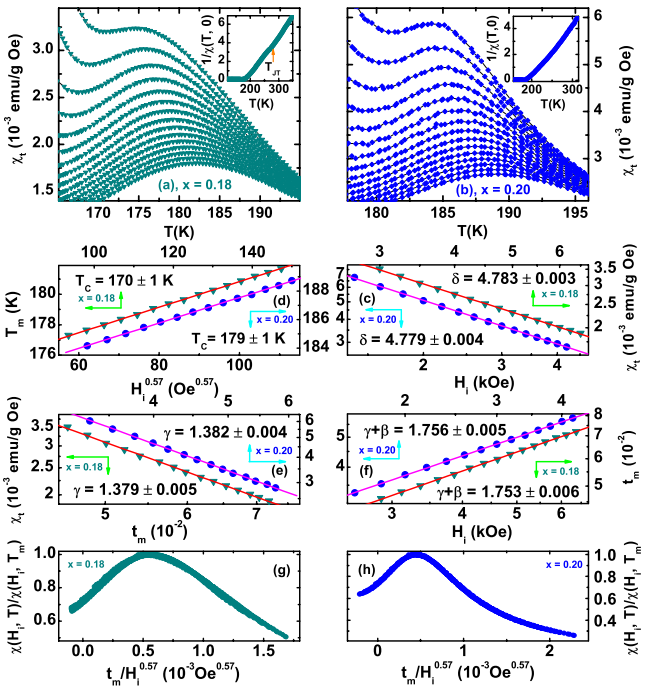

FIG. 2. (Color online) Main bodies of (a) (x=0.18) and (b) (x=0.20) are $\chi(H,T)$ (corrected for background and demagnetization effects) measured on warming following zero field cooling (ZFC) in various static fields, (a) from 5 (top) to 9 kOe (bottom) in 250 Oe steps and (b) from 1.4 (top) to 4.2 kOe (bottom) in 200 Oe steps. The insets show $1/\chi(H=0,T)$. (c) Plot of $\log(\chi_m)$ vs $\log(H_i)$ yielding the exponent δ. (d) Plot of T_m against $H_i^{0.57}$ yielding an estimate for T_C. (e) Plot of $\log(\chi_m)$ vs $\log(t_m)$ yielding the exponent γ. (f) Plot of $\log(t_m)$ vs $\log(H_i)$ yielding the exponent sum $\gamma+\beta$ and hence β. Susceptibility scaling plots for (g) x=0.18 and (f) x=0.20 using the data in (a) and (b).

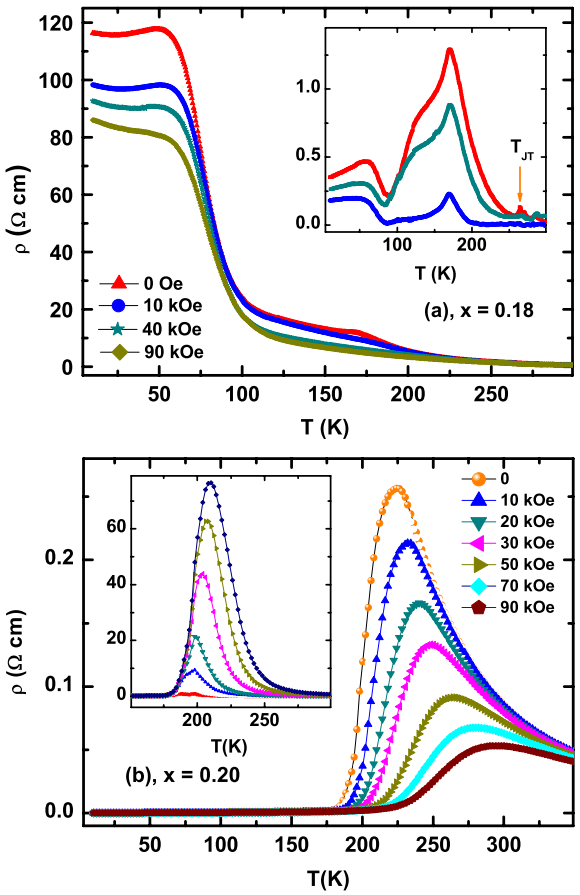

FIG. 3. (Color online) (a) Resistivity for x=0.18 measured on warming following ZFC; inset, the MR=$\Delta\rho/\rho(0)=[\rho(0)-\rho(H)]/\rho(0)$. (b) Same as (a) but for x=0.20, which exhibits CMR behavior.

terms of scaling law predictions, have been well documented previously,[14,17] so that a simple summary of those predictions are given here. First, the dependence of the ac susceptibility peak amplitude on field, $\chi_m(H_i,t_m)\sim H_i^{(1/\delta-1)}$, is tested in the log-log plot of Fig. 2(c), and yields δ=4.783±0.003 (x=0.18) and δ=4.779±0.004 (x=0.20) (estimates that are clearly independent of any choice for T_C). Second, the predicted power-law dependence of the (reduced) peak temperature on field, $t_m=(T_m-T_C)/T_C\sim H_i^{0.57}\sim H_i^{1/(\beta+\gamma)}$, is similarly reproduced in Fig. 2(d). Here an estimate for T_C is clearly required, and is furnished by plotting the measured T_m against $H_i^{0.57}$ and extrapolating to H_i=0 [viz., $(\gamma+\beta)^{-1}$ =0.57 for Heisenberg model exponents[18]], yielding T_C =170±1 K (x=0.18) and T_C=179±1 K (x=0.20). The latter are then used in double-logarithmic plots of t_m against $H_i^{1/(\beta+\gamma)}$ to yield self-consistently refined values[14,17] for $\gamma+\beta$ and T_C. Third, the dependence of peak amplitude on (reduced) temperature, $\chi_m(H_i,t_m)\sim t_m^{-\gamma}$, is similarly tested [Fig. 2(e)], yielding γ=1.379±0.005 and hence β =0.374±0.002 (x=0.18), and γ=1.382±0.004 and β =0.374±0.002 (x=0.20). A final test of the applicability of 3D Heisenberg model is provided in Figs. 2(g) and 2(h); scaling predicts that such $\chi(H,T)$, when normalized to their peak values $[\chi(H,T_m)]$, should fall on a universal curve when plotted against the argument $t_m/h^{1/(\gamma+\beta)}$ of the scaling function,[14,17] $h\sim H_i/T_C$ being the conventional linear scaling field.

That these samples straddle the compositional M-I boundary is confirmed by the magnetoresistivity (MR) data, $\rho(H,T)$, reproduced as a function of temperature in various applied fields, $0<H<90$ kOe, in Fig. 3(a) (x=0.18) and Fig. 3(b) (x=0.20). These data support the conclusion that this compositional threshold lies in the range $0.18\leq x_c\leq 0.22$.[5,7–10] In particular, the x=0.18 sample exhibits an insulating ground state [$\rho(H=0,T=10$ K)=116 Ω cm] above which there are three phase transitions: a structural transition at $T_B\approx 50$ K, a higher temperature FM-PM transition ≈170 K, and a JT transition at $T\approx 270$ K. The latter is also evident in the $1/\chi(0,T)$ vs T plot and corresponds to a pseudocubic-to-orthorhombic structural transition (coincident with a OO*-OO transition) (Refs. 10 and 11). In contrast, the x=0.20 specimen exhibits a metallic ground state [$\rho(H=0,T=10$ K)=1.85×10^{-4} Ω cm] close to a factor of 10^6 lower than that at x=0.18 with the associated FM-PM (M-I) transition ≈180 K. It also exhibits a strong field-dependent resistivity[5] characteristic of CMR systems.

The fundamental questions raised by the present results are: what coupling mechanisms underlie the establishment of a FM ground state across the compositional M-I transition and what, if any, is the relationship between them?

In answer to the first question, the present results confirm unequivocally that ferromagnetism is established *prior* to the emergence of metallicity. An immediate corollary to the latter is that a mechanism other than DE must control the ordering process in the insulating regime. As outlined in the introductory section, metallicity accompanies the establishment of an infinite percolating pathway of metallic—i.e., DE-linked sites; here ferromagnetism precedes metallicity. There is an emerging consensus that the relevant interaction initiating ferromagnetism in the *nonmetallic* (and thus non-DE-dominated) regime is superexchange (SE). This is based on the evolution of the sign/magnitude of SE with composition deduced from neutron-scattering data.[24] The parent compound, $LaMnO_3$, exhibits "in-plane" ferromagnetism, reflecting the fact that the corresponding in-plane SE coupling integral $J_{ab}>0$ and out-of-plane antiferromagnetic (AFM) SE coupling $J_c<0$, a magnetic structure induced/stabilized by OO (Ref. 25) [this structure can also be discussed in terms of the semiempirical Kanamori-Goodenough-Anderson rules,[6] in which the sign of SE coupling reflects the Mn-O-Mn bond angles and bond lengths]. These neutron data indicate that whereas the magnitude of the FM-SE in-plane coupling, $J_{ab}(x)$, increases monotonically with increasing doping level (x) over the range relevant to the present discussion, the c-axis coupling $J_c(x)$ evolves in a more complicated manner. Specifically, $J_c(x<0.125)<0$ and $J_c(x=0.125)=0$, whereas $J_c(0.125<x<0.22)>0$. This signals the emergence of a FM-SE c-axis coupling for $x>0.125$, the magnitude of which increases subsequently roughly linearly with x (for $x>0.125$).[24] Thus both $J_{ab}(x)$ and $J_c(x)$ are positive/FM in proximity to the compositionally induced metal-insulator transition in $La_{1-x}Ca_xMnO_3$, resulting in FM order being established in the attendant insulating regime. Specifically, an infinite/percolating backbone of FM-SE linked sites is established but this backbone is manifestly not conducting, thus SE, not metallicity controlling DE, is the predominant mechanism.

By contrast, in the adjacent metallic regime, the present data demonstrate that not only does this percolating backbone remain FM but it also becomes conducting. Correspondingly, DE must become the dominant mechanism as metallicity emerges. It should be realized that, however, once the FM percolation threshold is exceeded, further increases in hole doping will simply modulate the number of sites/spins coupled to this infinite backbone (and participating in the ordering process) *incrementally*. That is, from a statistical standpoint, the number of sites falling within the DE/SE near-neighbor coupling range of backbone will only increase marginally with increases in hole doping once the percolation threshold has been exceeded; Mn sites exceeding this coupling range remain decoupled from the backbone. It is the underlying interaction *mechanism* that is being changed in this regime. The implication, therefore, is that the critical amplitude, D_0, a measure of the number of moments participating in the ordering process (equivalently, the effective spin, S), should remain essentially unchanged in the insulating and metallic phases immediately adjacent to the compositionally driven M-I boundary, as is indeed observed experimentally. In contrast, attempts to answer the second question reveals some possibly unanticipated relationships between the differing mechanisms underlying ferromagnetism in this regime.

First, while Monte Carlo simulations conclude that the DE model—without anisotropy—lies in the same universality class as the isotropic Heisenberg model,[26] no such predictions currently exist for SE. The present measurements reveal that it, too, lies in the same class. Indirect support for this latter conclusion is provided by the use of the same model to fit the measured dispersion relation for magnetic excitations for $x<x_c$.[24] Thus, the *anisotropy* in SE coupling $[J_{ab}(x)\neq J_c(x)]$ in the insulating regime appears to play no major role, likely because the differences between $J_{ab}(x)$ and $J_c(x)$ at the composition studied are somewhat less than the relevant thermal-energy scale, k_BT_C. Similar conclusions must also apply to DE coupling that, in a *noncubic* environment, would be rendered anisotropic.

Second, and of more interest, is a comparison between the measured T_C values themselves. They increase by just 8 K between $x=0.18$ and $x=0.20$. With measurements of the critical amplitude D_0 revealing that the number of sites participating in the ordering process remains essentially constant over the compositional regime studied (the effective spin S is unchanged), and as T_C is a function of S and the relevant coupling strength J, the immediate inference is that the magnitude J of DE and SE coupling at compositions spanning the M-I boundary must be quite comparable.[27] This conclusion (that the relative magnitudes of OO-stabilized FM-SE coupling and DE coupling in the OO^* metallic regime bordering the M-I phase boundary are comparable) at first appears conveniently coincidental.[28] However, the similarity in values of the acoustic spin-wave stiffness, D, in these two specimens supports this assertion. Typically, $D=2JSa^2$ for interacting near-neighbor spins (S) with separation a in a cubic environment, J being the relevant SE or DE interaction; minor changes in D between these two regimes implies comparable values for J. Further investigation, through both detailed model calculations based on the percolative nature of the ferromagnetism involving these two mechanisms,[29] and experimentally by examining the variation in the critical temperature at a more closely spaced doping level (viz., dT_C/dx) across the M-I boundary (the focus of a planned future study) would help confirm this conclusion.

An important corollary to the above discussion is that the current data demonstrate unequivocally that, despite the often cited near-neighbor characteristics of both SE and DE, the relevant percolation thresholds for these two interactions are manifestly different in $La_{1-x}Ca_xMnO_3$. For a specific lattice structure, the interaction with a longer range reaches its percolation threshold before that with a shorter range. Thus SE-mediated FM coupling in the insulating phase ($x=0.18\leq x_c$) must necessarily be (slightly) longer than DE; if the converse were true, ferromagnetism and metallicity *would* emerge coincidentally.

Despite these and other differences, particularly, differences in the ground-state transport behavior by examining the MR in the paramagnetic (PM) regime, it is possible to compare the *high* temperature coupling between (partially) mobile e_g electrons and localized t_{2g} spins, as was done for $La_{1-x}Sr_xMnO_3$ near its M-I transition.[5,30] This comparison is

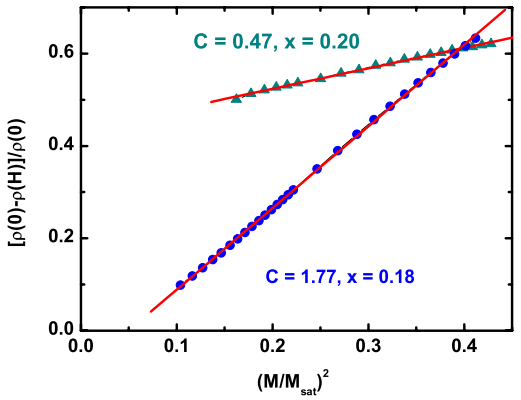

FIG. 4. (Color online) Scaling of the MR with M (at $T \approx 1.02T_C$ with $5<H<80$ kOe), using $\Delta\rho/\rho(0)=C(M/M_{sat})^2$.

based on the use of Ginzburg-Landau/mean-field predictions for the PM state,[30] viz., $\Delta\rho(H,T)/\rho(0)=C[M(H,T)/M_{sat}]^2$, where C represents the effective coupling between hopping e_g electrons and localized t_{2g} spins. This coupling constant depends on the ratio J_H/W, J_H being the Hund's coupling between itinerant and localized electrons and W the one-electron e_g bandwidth. This prediction is confirmed in Fig. 4 for data immediately above T_C (i.e., $T\approx 1.02T_C$), from which $C=1.77$ for $x=0.18$, considerably larger than the estimate of $C=0.47$ at $x=0.20$. This trend is consistent with that observed in $La_{1-x}Sr_xMnO_3$ and supports the conclusion that the value for C decreases as the hole concentration, n, is increased,[5,30] likely reflecting a significant decrease in the one-electron bandwidth, W, as the "insulating" phase is approached. Agreement with the above predictions at compositions displaying such an insulating ground state indicates that even in the case of (partially) localized e_g spins (viz., in the absence of a percolating backbone of DE-linked e_g electron hopping pathways), magnetism and conduction remain strongly coupled in the PM regime.

IV. SUMMARY AND CONCLUSIONS

In summary, detailed measurements of the critical temperatures, exponents, and amplitudes in two $La_{1-x}Ca_xMnO_3$ single crystals spanning the compositionally driven M-I boundary are presented. It is argued that the similarities in these critical parameters demonstrate (i) that once an infinite percolating backbone of OO-stabilized FM-SE linked sites has been established in the insulating phase, no significant increase in the number of sites/spins participating in the ordering process occurs on crossing into the adjacent, DE-dominated OO* metallic regime; (ii) the FM percolation threshold for these interactions are slightly, but clearly, different despite the often said assumption that both forms of coupling are essentially near neighbor and thus comparable; (iii) OO-stabilized FM-SE and DE must possess quite comparable magnitudes at compositions close to the M-I boundary. This picture differs significantly from models describing CMR in this system[5] based on phase separation into AFM insulating and FM conducting regions. There is, however, no conflict between the latter and the conclusions reached above. Here OO-stabilized FM-SE dominates the magnetic response of insulating regime bordering the compositionally modulated M-I boundary. However, the transition to an (OO*) state, which accompanies the emergence of the metallic phase in which DE dominates,[11] destabilizes FM-SE, replacing it with its AFM counterpart prevalent in the undoped parent compound.

ACKNOWLEDGMENTS

We thank J. Neumeier, A. Millis, and J. S. Zhou for helpful discussions. Support for this work by the Natural Sciences and Engineering Research Council (NSERC) of Canada, the University of Manitoba (via a graduate scholarship to WJ), and MISIS is gratefully acknowledged.

*jiang@physics.umanitoba.ca

[1] M. Imada, A. Fujimori, and Y. Tokura, Rev. Mod. Phys. **70**, 1039 (1998).
[2] T. Okuda, A. Asamitsu, Y. Tomioka, T. Kimura, Y. Taguchi, and Y. Tokura, Phys. Rev. Lett. **81**, 3203 (1998).
[3] P. Schiffer, A. P. Ramirez, W. Bao, and S.-W. Cheong, Phys. Rev. Lett. **75**, 3336 (1995).
[4] T. Okuda, Y. Tomioka, A. Asamitsu, and Y. Tokura, Phys. Rev. B **61**, 8009 (2000).
[5] See, for example, *Colossal Magnetoresistive Oxides*, edited by Y. Tokura (Gordon and Breach Science, New York, 2000); *Nanoscale Phase Separation and Colossal Magnetoresistance*, edited by E. Dagotto (Springer, Berlin, 2002); J. M. D. Coey, M. Viret, and S. V. Molnar, Adv. Phys. **48**, 167 (1999).
[6] C. Zener, Phys. Rev. **81**, 440 (1951); P. W. Anderson and H. Hasegawa, *ibid.* **100**, 675 (1955).
[7] G. Biotteau, M. Hennion, F. Moussa, J. Rodríguez-Carvajal, L. Pinsard, A. Revcolevschi, Y. M. Mukovskii, and D. Shulyatev, Phys. Rev. B **64**, 104421 (2001).
[8] Pengcheng Dai, J. A. Fernandez-Baca, E. W. Plummer, Y. Tomioka, and Y. Tokura, Phys. Rev. B **64**, 224429 (2001); Pengcheng Dai, J. A. Fernandez-Baca, N. Wakabayashi, E. W. Plummer, Y. Tomioka, and Y. Tokura, Phys. Rev. Lett. **85**, 2553 (2000).
[9] E. S. Božin, M. Schmidt, A. J. DeConinck, G. Paglia, J. F. Mitchell, T. Chatterji, P. G. Radaelli, Th. Proffen, and S. J. L. Billinge, Phys. Rev. Lett. **98**, 137203 (2007).
[10] S. J. L. Billinge, R. G. DiFrancesco, G. H. Kwei, J. J. Neumeier, and J. D. Thompson, Phys. Rev. Lett. **77**, 715 (1996); C. H. Booth, F. Bridges, G. H. Kwei, J. M. Lawrence, A. L. Cornelius, and J. J. Neumeier, *ibid.* **80**, 853 (1998); Y. Jiang, F. Bridges, L. Downward, and J. J. Neumeier, Phys. Rev. B **76**, 224428 (2007).
[11] Bas B. Van Aken, Oana D. Jurchescu, Auke Meetsma, Y. Tomioka, Y. Tokura, and Thomas T. M. Palstra, Phys. Rev. Lett. **90**, 066403 (2003).

[12] C. Lin and A. J. Millis, Phys. Rev. B **78**, 174419 (2008).
[13] D. Shulyatev, S. Karabashev, A. Arsenov, Y. Mukovskii, and S. Zverkov, J. Cryst. Growth **237-239**, 810 (2002).
[14] J. H. Zhao, H. P. Kunkel, and X. Z. Zhou, Gwyn Williams, and M. A. Subramanian, Phys. Rev. Lett. **83**, 219 (1999); Wanjun Jiang, X. Z. Zhou, Gwyn Williams, Y. Mukovskii, and K. Glazyrin, Phys. Rev. B **78**, 144409 (2008); G. Williams, J. Alloys Compd., **326**, 36, (2001).
[15] A. Arrott, Phys. Rev. **108**, 1394 (1957).
[16] A. Arrott and J. E. Noakes, Phys. Rev. Lett. **19**, 786 (1967).
[17] H. E. Stanley, *Introduction to Phase Transitions and Critical Phenomena* (Clarendon, Oxford, 1971).
[18] M. Campostrini, M. Hasenbusch, A. Pelissetto, P. Rossi, and E. Vicari, Phys. Rev. B **65**, 144520 (2002).
[19] S. N. Kaul, Phys. Rev. B **24**, 6550 (1981).
[20] Wanjun Jiang, X. Z. Zhou, Gwyn Williams, Y. Mukovskii, and K. Glazyrin, Phys. Rev. Lett. **99**, 177203 (2007); Wanjun Jiang, X. Z. Zhou, G. Williams, Y. Mukovskii, and K. Glazyrin, Phys. Rev. B **76**, 092404 (2007).
[21] K. Ghosh, C. J. Lobb, R. L. Greene, S. G. Karabashev, D. A. Shulyatev, A. A. Arsenov, and Y. Mukovskii, Phys. Rev. Lett. **81**, 4740 (1998); D. Kim, B. L. Zink, F. Hellman, and J. M. D. Coey, Phys. Rev. B **65**, 214424 (2002); Wei Li, H. P. Kunkel, X. Z. Zhou, Gwyn Williams, Y. Mukovskii, and D. Shulyatev, *ibid.* **70**, 214413 (2004).
[22] F. Keffer, *Spin Waves (Handbuch der Physik, VIII/2)* (Springer, Berlin, 1966).
[23] T. Brown, Wei Li, H. P. Kunkel, X. Z. Zhou, Gwyn Williams, Y. Mukovskii, and A. Arsenov, J. Phys.: Condens. Matter **17**, 5997 (2005).
[24] M. Hennion, F. Moussa, P. Lehouelleur, F. Wang, A. Ivanov, Y. M. Mukovskii, and D. Shulyatev, Phys. Rev. Lett. **94**, 057006 (2005).
[25] Y. Tokura and N. Nagaosa, Science **288**, 462 (2000).
[26] Y. Motome, and N. Furukawa, J. Phys. Soc. Jpn. **68** 3853 (1999); **69** 3785, (2000); **70**, 1487, (2001); L. Alonso, L. A. Fernández, F. Guinea, V. Laliena, and V. Martín-Mayor, Nucl. Phys. B **596**, 587 (2001).
[27] B. R. Coles, B. V. B. Sarkissian, and R. H. Taylor, Philos. Mag. B **37**, 489 (1978).
[28] G. Papavassiliou, M. Pissas, M. Belesi, M. Fardis, J. Dolinsek, C. Dimitropoulos, and J. P. Ansermet, Phys. Rev. Lett. **91**, 147205 (2003).
[29] T. V. Ramakrishnan, H. R. Krishnamurthy, S. R. Hassan, and G. Venketeswara Pai, Phys. Rev. Lett. **92**, 157203 (2004).
[30] A. Urushibara, Y. Moritomo, T. Arima, A. Asamitsu, G. Kido, and Y. Tokura, Phys. Rev. B **51**, 14103 (1995).